Links between ocean deoxygenation and phytoplankton evolution in an Early Jurassic greenhouse world: A palynological study of Lowermost Hettangian black shales from southwest England.

MSc thesis by Nikki Szerkowski (3585514)

Supervised by dr. Bas van de Schootbrugge and dr. Sander Houben

November 2016

Utrecht University

Abstract

The end of the Triassic is characterized by a large mass extinction event, were approximately 80% of all species became extinct. The extinction event was caused by extensive volcanism from the Central Atlantic Magmatic Province (CAMP; ~201 Ma) which lead to global warming and caused an oxygen deficiency and euxinic conditions in the oceans. The loss of oxygen also coincided with a shift from red algae towards green algae. Here, we present a composite succession of four sections (Lilstock, Kilve, East-Quantoxhead and St. Audrie's Bay) from south-west England covering the entire Hettangian stage using a high-resolution quantative analysis of 50 samples providing information on both marine and terrestrial palynomorphs. The Hettangian was characterized by mainly green algae (acritarchs and prasinophytes) but has several episodes were red algae (dinoflagellates) became more abundant. This could mean that the entire Hettangian still experienced dysoxic conditions with several episodes with more oxic conditions. Abundances of Structureless Organic Matter (SOM) and pyrite suggest that the Hettangian also knew episodes of Photic Zone Euxinia (PZE). The biodiversity was low for terrestrial palynomorphs (pollen and spores), but it fluctuated for marine algae, which might indicate more dynamic changes in stratification and redox conditions in the oceans. These changes might be orbitally forced. Ongoing anoxic conditions in the oceans were driven by late-stage eruptive phases of CAMP volcanism, which continued for at least 600 kyr after the Triassic-Jurassic boundary but based on this results are thought to continue up into the Sinemurian.

Table of contents

1. Introduction

During the early Mesozoic the Earth consisted of one supercontinent named Pangea and the entire Earth's continental crust resided at one side off the globe (Figure 1). Considering the enormous size of the supercontinent an extensive part of the land was far away from the Earth's oceans resulting in a dry climate at the centre of the landmass. Due to the Earth's property that landmasses have a lower heat capacity than oceans, the interior of the continent experienced strong seasonality, with very hot summers and cool winters. These huge temperature differences between northern and southern hemisphere lead to pressure differences and therefore creating strong cross-equatorial monsoonal winds. (Stanley, 2009)

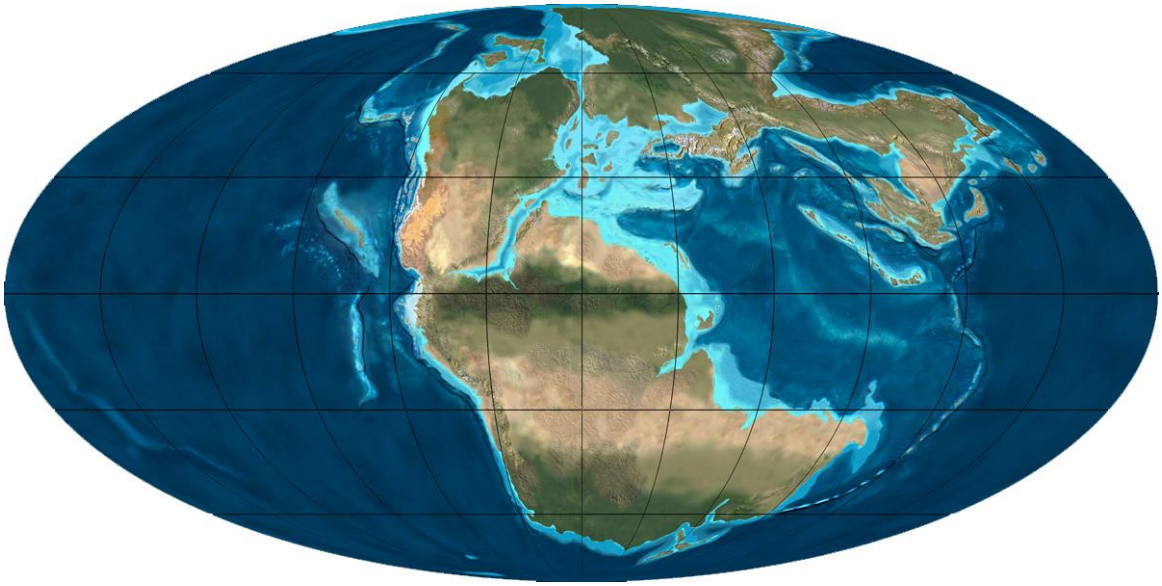

Figure 1, Geography of the Early Jurassic (Figure from: ©Ron Blakey, Colorado Plateau Geosystems)

The Earth has known at least five periods with major extinction events, one of which occurred just before the Triassic-Jurassic boundary (Newell, 1963; Raup & Sepkoski, 1982; Tanner et al., 2004). This extinction event, the End Triassic Extinction (ETE), occurred around 201.6 Ma ago (Blackburn et al., 2013) and approximately 80% of all of the species became extinct (Sepkowski, 1996). Several reasons are proposed to have caused the ETE. For example, Olsen (2002) suggested a bolide impact as he found both an iridium anomaly and fern spike around the Triassic-Jurassic boundary. However, Tanner et al. (2004) states that evidence for this suggestion is not found globally and that the iridium anomaly also could be volcanically induced. Also the exact timing of such an event at the Triassic-Jurassic boundary is lacking. Sea-level fluctuations are a second proposed cause for the large extinction event. Hallam (1997) and Hallam & Wignall (1997) found that the timing of the extinction coincided with a regression phase. Nonetheless, other periods with regression do not necessarily coincide with extinction phases and the regression at the end Triassic seems to be a regional feature instead of global situation (Hallam, 1990, 1998, Hallam et al., 2000; Tanner et al., 2004).

The base for the most substantiated cause of the ETE was made by McHone (1996), who found similarities in both the composition and age of basalt rocks from North America and suggests

that there was a large flood basalt province during the Early Jurassic, which coincided with the breakup of the supercontinent Pangea. Marzoli et al. (1999) extended this province (Figure 2), and discovered that it covers large parts of North and South America, Iberia and Africa and they named it Central Atlantic Magmatic Province (CAMP). Further proof for the CAMP theory is derived from an increase in leaf stomata (McElwain et al., 1999) which coincides with the ETE, suggesting an approximate 4-fold increase in ρCO_2, from 600ppm to approximately 2400 ppm.

Pálfy et al. (2001) established a record with a compelling negative $\delta^{13}C$ isotope excursion in both marine carbonates and organic carbon around the Triassic-Jurassic boundary in Hungary and similar isotope excursions were also found for marine organic matter in St. Audries Bay (Hesselbo et al., 2002) and at the Queen Charlotte Islands (Ward et al., 2001). Hesselbo et al. (2002) concludes that this input of lighter carbon is linked to CO_2 outgassing due to CAMP volcanism, but it is feasible that it is induced by gas hydrates. However, gas hydrates are eliminated as a true cause for the ETE by a mismatch between the extinction event and the negative $\delta^{13}C$ isotope excursion that is linked to methane release, this suggests that they were more likely a consequence of the reason for the ETE than a cause (Ruhl et al., 2011; van de Schootbrugge et al., 2013). Hesselbo et al. (2002) found that disturbed carbon isotopes, and therefore CO_2 outgassing due to CAMP volcanism, persisted for at least 600 kyr after the initial excursion. Eventually Blackburn et al. (2013) links the ETE precisely to CAMP volcanism using zircon U-PB geochronology on numerous CAMP flows and intrusions, hereby dating four different CAMP eruptions and their corresponding pulses of CO_2 release over a period of 600 kyr.

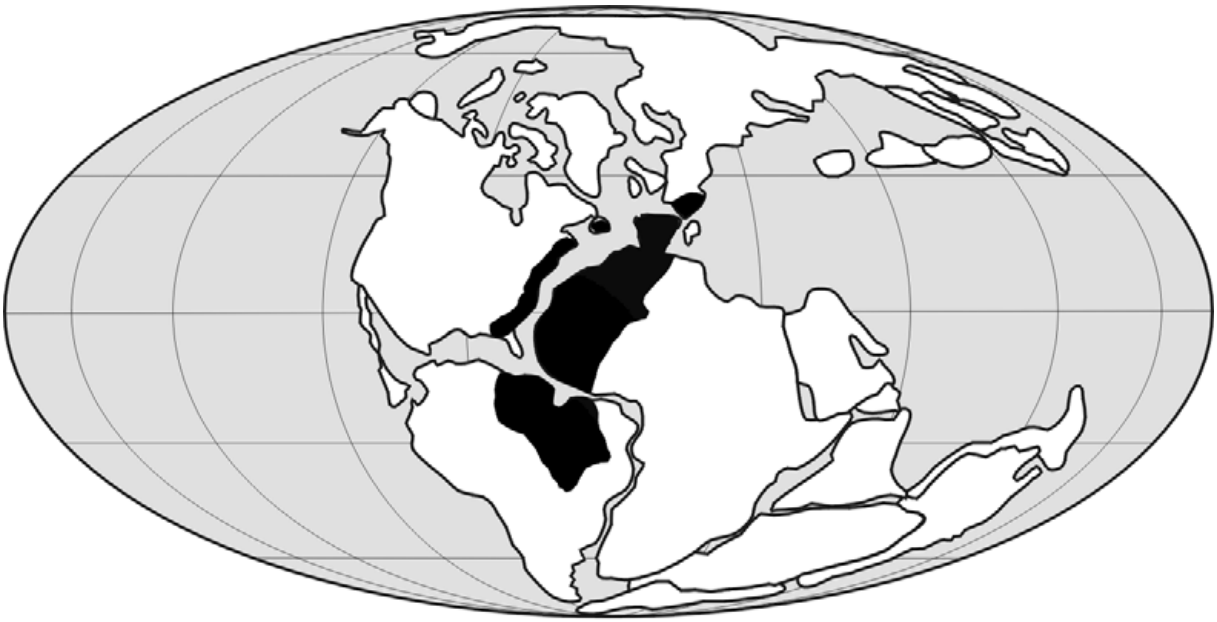

Figure 2, Extension of CAMP volcanism (Figure from Tanner et al., 2004)

The proposed rise in ρCO_2 at the end of the Triassic has multiple effects on the Earth's Climate. First, an input of CO_2 in the Earth's atmosphere also leads to an increased uptake of CO_2 by the oceans, hereby causing ocean acidification (Beerling and Berner, 2002; Hautmann et al.,

2008). Secondly, CO_2 is a greenhouse gas and therefore it is a trigger for global warming. McElwain (1999) already predicted that the rise in CO_2 is equivalent to a global temperature rise of approximately 3-4°C. Oyster data also provides us with a sea surface temperature change of approximately ~4°C, and also with a decrease in salinity of 3PSU attributed to an enhanced hydrological cycle. An increase of fresh water results in stratification of the water column and therefore anoxic ocean water conditions (van de Schootbrugge et al., 2007).

At the ETE a shift from red algae towards a green algal proliferation is observed (Falkowski et al., 2004; van de Schootbrugge et al., 2007) indicating a link between anoxia and green algae (van de Schootbrugge et al., 2007). The discovery of isorenieratane right after the ETE is evidence for the presence of Green Sulphur Bacteria (GSB) and this, along with paper shales, pyrite framboids and no benthic activity, indicates that there must have been Photic Zone Euxinia (PZE) (Damsté et al., 2001; Richoz et al., 2012; Jaraula et al., 2013; van de Schootbrugge et al., 2013). A change in $\delta^{15}N$ and trace elements also suggest an overturning of the redox conditions of the oceans (Richoz et al., 2012) and a change in $\delta^{34}S$ suggests the abundance of free H_2S in the water column (Jaraula et al., 2013). Kasprak et al. (2015) found that these stressed marine conditions were not restricted to the European Epicontinental Sea (EES) but that it is presumable that PZE was a global event. An increase of ammonium in Hettangian oceans due to the overturning redox conditions may have favoured green algae which have a higher uptake quotient than red algae (Litchman et al., 2006). The aryl isoprenoid ratio suggests that episodic PZE possibly extended into the Early Jurassic (Jaraula et al., 2013).

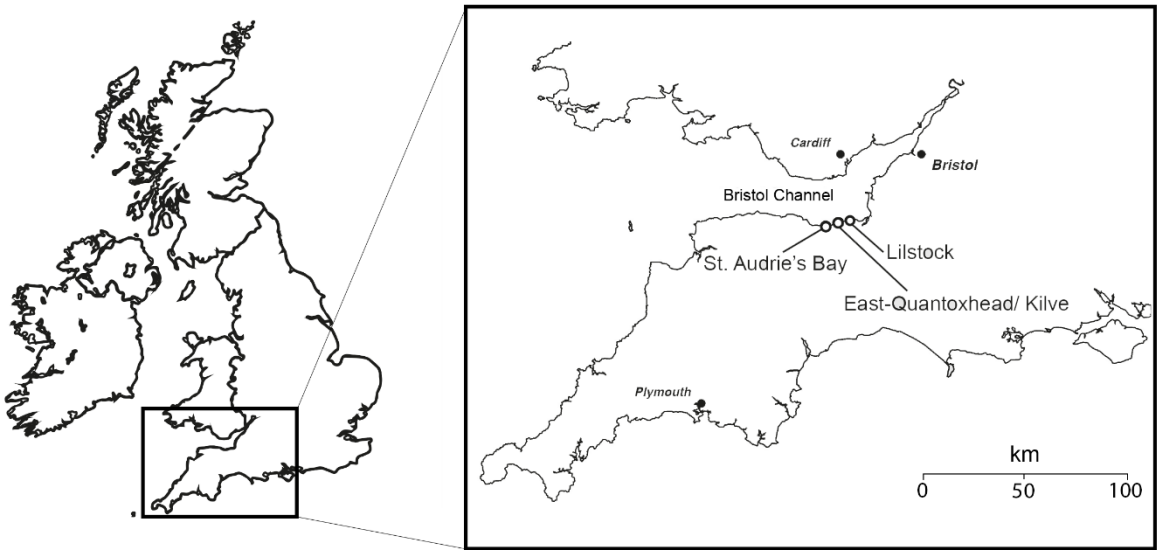

Figure 3, The location of the studied outcrops along the Somerset coast in southwest England

For this thesis, 77 meters of an approximately 120 meter succession along the Somerset Jurassic coast in SW England (Figure 3) were studied, which is known to cover the entire Hettangian stage (Ruhl et al., 2010). This research starts just above the base of the Hettangian and extends into the lower Sinemurian. A palynological study was performed on both marine and terrestrial palynomorphs, providing insight in the recovery after the ETE. The aim of this study is to find links between ocean deoxygenation and phytoplankton evolution in the Early

Jurassic, therefore, several aspects were examined. 1) The relative number of palynomorphs within the marine and terrestrial groups provide insight in how both the communities recover. 2) Absolute numbers of palynomorphs were compared with pyrite content and amorphous organic matter (AOM) to display variations in deposition and/or preservation, therefore providing information on the water column conditions. 3) Spectral analysis was preformed to obtain insights in the driving mechanism behind population fluctuations during recovery. 4) Biodiversity indices were determined to find out how the palynomorph populations are recovering. 5) The Sporomorph EcoGroup (SEG) model (Abbink, 1998) provides insight on climate recovery in the terrestrial environment.

2. Background information

2.1 Geological history

2.1.1 Paleo-environment and stratigraphy

At the time of deposition, the study area was situated in the western Tethys realm (Figure 4) and was surrounded by Pangean landmasses, making it part of the EES. Prior to the Hettangian, the end of the Triassic the marine environment at this location was characterized by a series of environmental changes (Ruhl et al., 2010), which are listed below. The end-Triassic Blue Anchor Fm. (Figure 5) had a shallow marine depositional environment (Warrington et al., 2008). The Blue Anchor Fm. is succeeded by the Westbury Fm., which shows fluctuations in relative sea level (Hesselbo et al., 2004). The subsequent Lilstock Fm. shows a shallowing environment (Wignall and Bond, 2008), and indicates emergence, reflected by an erosional surface (Hallam and Wignall, 1999; Hesselbo et al., 2004; Warrington et al., 2008) and again flooding to a lagoonal environment (Warrington et al., 2008) or carbonate ramp (Hesselbo et al., 2004). At last, the Blue Lias Fm. was deposited during long-term sea level rise during the Early Jurassic (Ruhl et al., 2010).

Figure 4, Location of SW England during the Early Jurassic, with the arrow indicating the studied location (Figure from: ©Ron Blakey, Colorado Plateau Geosystems)

2.1.2 Lithology

A detailed lithological representation of the stratigraphic succession along the Somerset coastline at St. Audrie's Bay and Quantoxhead, SW England can be found in Figure 5 and was established by Ruhl et al. (2010). The lithology consists of alternating homogeneous and inhomogeneous limestones with marls and shales. The limestones are often 10 to 20 cm thick, mud- or wackestones but can become up to 50 cm in extreme cases. They contain clay of various types, suggesting an undisturbed sedimentation from suspended particles (Paul et al., 2008). However, some of the limestone layers are diagenetically altered, creating lateral irregular beds (Ruhl et al., 2010). The limestones alternate with siliciclastic marls and shales varying from several centimeters up to a few meters. The marls and shales consist of a variation between pale-grey marls, dark-grey marls and organic rich laminated black shales (Paul et al., 2008). The different beds seem to change rhythmically, from black shales to dark-grey marls to pale-grey marls to a limestone bed and back to dark shales and marls (Paul et al., 2008). The alternations are influenced by orbital forcing and each alternation was suggested to represent a ~20 kyr precession cycle (Weedon et al., 1999) whereas the structural differences within the limestone beds represent a ~100 kyr eccentricity cycle (Paul et al., 2008).

2.2 Astronomical cyclicity in the Hettangian

For the correlation between different key-sections of the Hettangian and a reconstruction of the rate at which the palynological community during the Hettangian recovered it is crucial to have an accurate timescale. Estimates on both the timing of the Triassic-Jurassic boundary as well as the duration of the Hettangian widely vary, creating difficulties in understanding those issues. Combining lithology, physical and chemical proxies and applying astronomical proxies, Ruhl et al. (2010) established an astronomical timescale for the End-Triassic and Early Jurassic. Time series analysis of the proxy records and lithology show fluctuations on a 3.8-5.8-meter scale and within each oscillation they determined 3-5 black shale horizons. The 3.8-5.8-meter scale oscillations are proposed to be orbitally forced 100 kyr eccentricity cycles and the black shale horizons are believed to be orbitally forced precession cycles. Therefore, they determined that the Hettangian stage lasted for at least 18 eccentricity cycles and thus approximately 1.8 Myr. Hüsing et al. (2014) extended this sequence with 14 meters and, for that interval, established the same pattern as Ruhl et al. (2010). Magnetostratigraphy was additionally used for improved global correlation, since the timing of those events should be synchronous all over the world. Hüsing et al. (2014) combined all data with a new astronomical solution, La2010 (Laskar et al., 2011a) and only looked at the 405 kyr eccentricity cycle, since it is more stable in the chaos of the solar system than the 100 kyr eccentricity cycle and thus more reliable (Laskar et al., 2011a, 2011b). This approach matched well with the U-Pb calibrations of the Hettangian stage (Blackburn et al., 2013; Hüsing et al., 2014) and provided a slightly shorter duration of the Hettangian of 1.7 Myr.

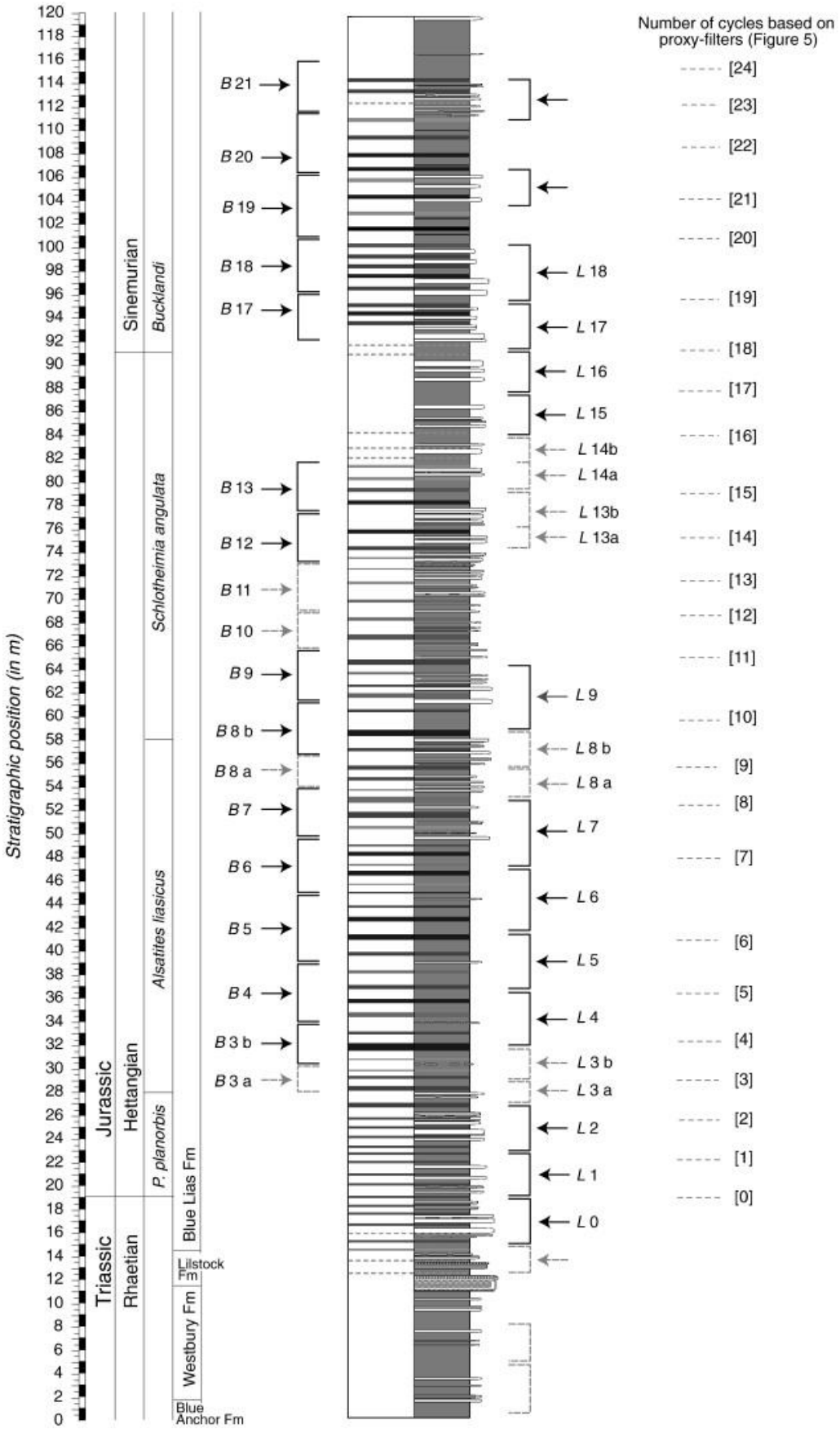

Figure 5, Lithology of the sedimentary stratigraphy sequence of southwest England (Figure from Ruhl et al., 2010)

2.3 Sporomorph EcoGroup model

In order to establish a proper interpretation of the terrestrial environment of the Jurassic and how it changed through time, Abbink (1998) and Abbink et al. (2004) conceived the Sporomorph EcoGroup (SEG) model. The SEG model is based on recent vegetation distribution and the integration of environmentally significant paleobotanical and palynological information. Variations in the stress-and disturbance level of species result in three different plant strategies. 1) A competitive strategy (low stress, low disturbance). 2) A stress tolerating strategy (high stress, low disturbance). 3) A ruderal strategy (low stress, high disturbance). These strategies result in six SEGs (Table 1, Figure 6) (Abbink, 1998; Abbink et al., 2004).

SEG	**Description**
Upland	Vegetation on higher terrain, well above groundwater level that is never submerged by water. A lack of fresh water and nutrients result in increased stress levels.
Lowland	Vegetation on plains and/or fresh water swamps; the plains may be periodically submerged by fresh water, resulting in the presence of 'wetter' or 'drier' species. There is an optimum in fresh water and nutrients resulting in low stress and low disturbance levels.
River	Vegetation on river banks which are submerged and subject of erosion. River species maintain a ruderal strategy.
Pioneer	Vegetation at instable and recently developed ecospace. Pioneer species maintain a ruderal strategy.
Coastal	Vegetation growing immediately along the coast, never submerged by the sea but under a constant influence of salt spray. Coastal species are under constant stress due to salt water.
Tidally-influenced	Vegetation that is daily influenced by tidal changes. Tidally-influenced species are under constant stress due to salt water.

Tabel 1, Description of the six different SEGs defined by Abbink (1998; et al., 2004)

Changes in the relative abundance of the different SEGs are expected to reflect changes in geography and climate. The ratio between Coastal SEG and Lowland SEG is indicative for sea level fluctuations. Variations within lowland SEG suggest climate change when plotting wet vs dry (humidity) elements or warm vs cold (temperature) elements (Abbink et al., 2004).

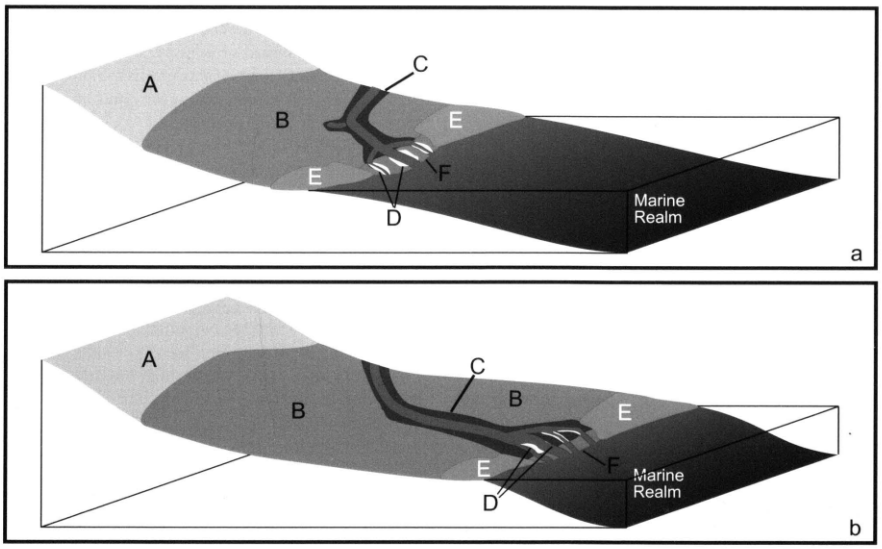

Figure 6, Schematic representation of the spatial distribution of the different SEG during a higher(a) and lower(b) sea-level. Upland (A), Lowland (B), River (C), Pioneer (D), Coastal (E) and Tidally-influenced (F) (Figure from Abbink et al., 2004).

3. Material and Methods

3.1 Location

A total of 50 samples were studied for this research project covering the Early Jurassic in South-West England (Figure 3). Samples were taken at an average 1-2 meter interval along the Somerset coast at Lilstock (9 samples) (51°12'02.9"N 3°10'36.9"W), St. Audries Bay (29 samples) (51°10'54.6"N 3°17'10.9"W) and Kilve (3 samples) (51°11'33.3"N 3°13'38.4"W), and were combined into one composite section. Also, 9 samples were used from an earlier fieldtrip performed by Micha Ruhl at St. Audries Bay and East-Quantoxhead to cover a missing interval.

3.2 Palynological processing and analysis

Palynological processing was performed at the Laboratory of Paleobotany and Palynology located at the Gemeenschappelijk Milieulaboratorium (GML), Utrecht University, the Netherlands. The samples were scraped for fresh sediment and crushed into small pieces. Approximately 5 grams of dried sediment was used for every sample and one lycopodium tablet (batch 1031) was added for absolute calculations of the results. The samples were rinsed once with 10% HCl for carbonate removal. Then the samples were rinsed with HF and shaken for two hours for the removal of silicates, two times in total. Afterwards, the samples were rinsed with 30% HCl and finally with water. Samples were sieved on 250 µm and 10 µm to remove both coarse and finest materials, and placed in an ultrasonic bath to break up bigger pieces. A homogenous quantity of sample together with glycerine jelly was transferred to a microscope slide and finally varnished. The remaining organic material was transferred to small vials for storage.

The slides were analysed on two different microscopes. 1) Slides low on amorphous organic matter were studied at Utrecht University with a Leica Laborlux D microscope, with a 10x40

and 10x63 magnification. 2) Slides high on amorphous organic matter were studied at TNO Utrecht with a Leica DMR microscope, with a 10x40 and 10x63 magnification. Here, samples were studied both in regular light and ultraviolet light for accurate counting of the specimens enclosed within amorphous organic material.

A total of approximately 300 palynomorphs per slide were counted on a species level for acritarchs, dinoflagellates, prasinophytes, pollen and spores. Identification of the different species was based on Wall (1965), Bonis et al. (2009) and Heunisch et al. (2010). Apart from this, individual lycopodium spores were counted for calculations on absolute abundances. Photographs of the palynomorphs are found in the Appendix (1: acritarchs, 2: dinoflagellates, 3: prasinophytes, 4: pollen, 5: spores).

3.3 Biodiversity

Calculations for biodiversity were made for species richness (S), species evenness (J) and the Shannon index (H) using the multivariate statistics software Primer. The species richness is the total number of different species. The species evenness is a measure for homogeneity of abundances of different species. The evenness is a value between zero and one, with zero meaning a lot of variety and one meaning little variation (Mulder et al., 2004; Cowell, 2009). The Shannon index is a measure for diversity based on a communication theory which is derived from the principle of how to predict the next letter in a message, where the uncertainty is measured by the Shannon Function 'H' ($H = -\sum_{i=1}^{n} \rho i \ \ln \rho i$). The index is combining both the richness and evenness. Values around 3-4 indicate a healthy population, below that the biodiversity is low (Shannon, 1948; Shannon & Weaver, 1949; Spellerberg & Fedor, 2003; Cowell, 2009).

3.4 Spectral analysis

Frequency analysis was performed on different groups of phytoplankton using the AnalySeries 1.1.1. program (Paillard et al., 1996). Before analysing, the linear trend was removed from the data. Then a Blackman-Tukey frequency analysis was performed using default settings with a Bartlett window and an 80% confidence interval. Presented power spectra are notified in m/cycle.

4. Results

4.1 Biostratigraphy

Figure 7 shows the stratigraphic range of all palynomorphs that were recovered from the composite section. The palynomorphs are divided in five groups (acritarchs, dinoflagellates, prasinophytes, pollen and spores) and arranged on both their first and last occurrences in these samples.

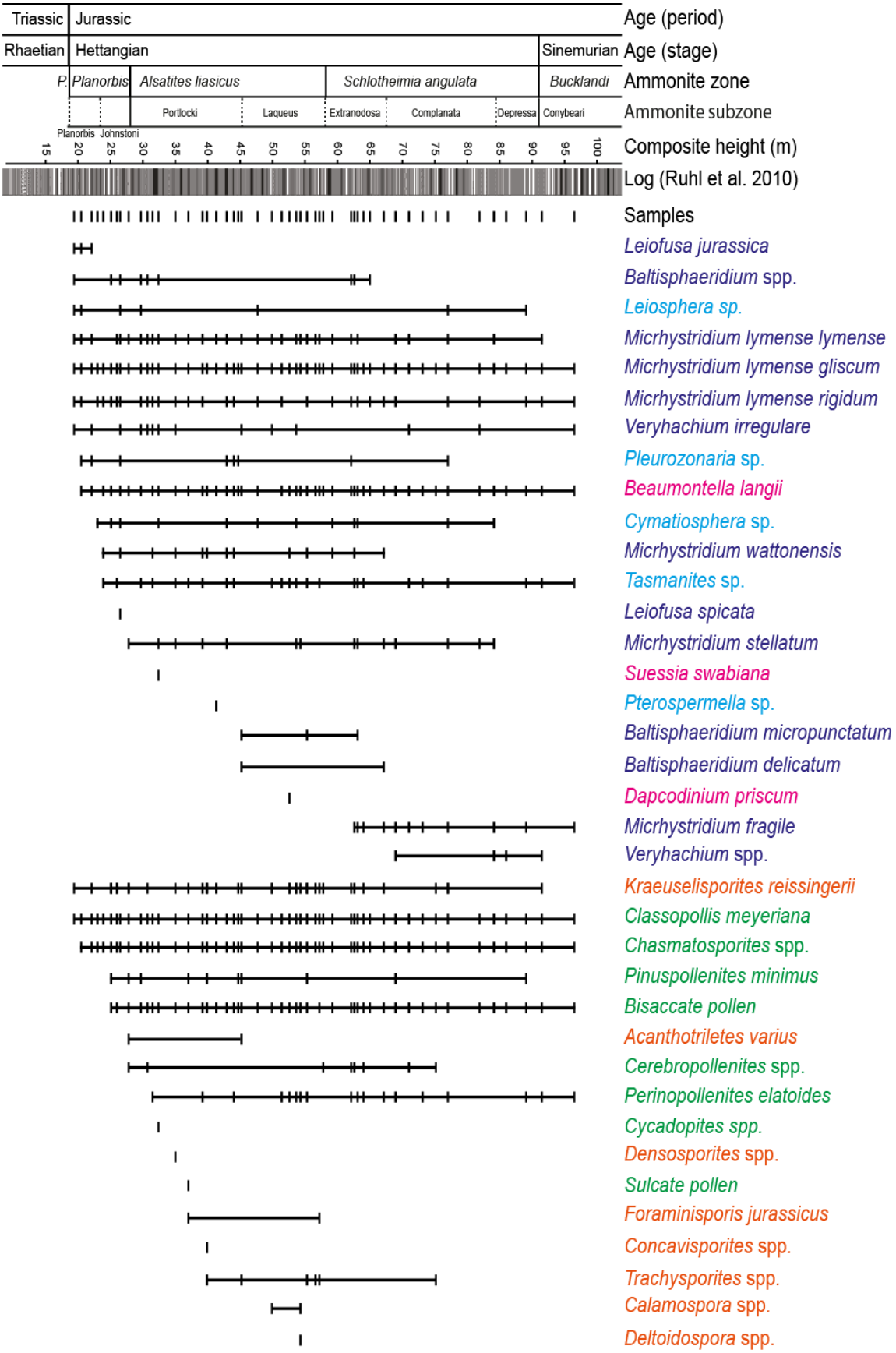

Figure 7, Stratigraphic range of all species sorted on both their first and their last occurrence in the studied sample set. Marine species: acritarchs (dark-blue), dinoflagellates (pink), prasinophytes (light-blue). Terrestrial species: pollen (green) and spores (orange).

4.1.1 Marine

Within the acritarchs, *Micrhystridium lymense rigidum, Micrhystridium lymense gliscum, Micrhystridium lymense lymense* and *Veryhachium irregulare* are abundant through the entire interval. Other *Micrhystridium* species and also *Baltisphaeridium* spp. seem to have stratigraphic ranges for this period. *Micrhystridium wattonensis* has a range from just after the *planorbis* and *johnstoni* ammonite subzones boundary (23.9 m) till the boundary between the *extranodosa* and *complanata* subzone (67.1 m). *Micrhystridium stellatum* ranges from the *johnstoni* and *portlocki* subzone boundary (27.8 m) till the boundary between the *complanata* and *depressa* subzone (84.1 m). *Micrhystridium fragile* has a first occurrence at 62.6 m and ranges to the top of the section. *Baltisphaeridium* spp. is present in the first samples and can be detected up to the *extranodosa* and *complanata* subzone boundary (67.1 m). *Leiofusa jurassica* is very abundant at the base of the succession and rapidly declines until it has a last occurrence at 22.1 m, just before the boundary between the *planorbis* and *johnstoni* subzones. *Leiofusa spicata*, *Baltisphaeridium delicatum* and *Baltisphaeridium micropunctatum* only occur incidentally. In the dinoflagellate group, *Beaumontella langii* is not present in all of the lowermost samples but they are detected over the entire interval. Other dinoflagellate species, *Suessia swabiana* and *Dapcodinium priscum,* were only observed once. Various types of prasinophytes were found over the entire interval but they do not seem to show a specific range. *Pleurozonaria* sp. is first detected at 20.5 m and ranges till 77.03 m. *Cymatiosphaera* sp. and *Tasmanites* sp. appear after the *planorbis* and *johnstoni* ammonite subzone boundary. *Tasmanites* sp. has the most common occurrence of all prasinophytes.

4.1.2 Terrestrial

The samples also contain several terrestrial pollen and spores. *Classopollis meyeriana* ranges over the entire interval. *Chasmatosporites* spp. has its first occurrence at 20.5 m*, Bisaccate pollen* and also *Pinuspollenites minimus* are first detected at 25.1 m and *Perinopollenites elatoides* has its first occurrence at 31.5 m, all species are abundant in the remaining part of the succession. *Cerebropollenites* spp. has a range from 28.8 m and has a last occurrence at 75.2 m. Cycadopites spp. and Sulcate pollen were only detected once. All first occurrences and ranges do not seem to correlate to any ammonite subzones. The only spore ranging over more or less the entire interval is *Kraeuselisporites reissingerii*. All other spores, *Acanthotriletes varius*, *Densosporites* spp., *Foraminisporis jurassicus*, *Trachysporites* spp., *Concavisporites* spp., *Calamospora* spp. and *Deltoidospora* spp. only occurred incidentally.

4.2 Relative Marine record

Figure 8 shows the relative abundances of the marine palynomorphs compared to the $\delta^{13}C$ values and Total Organic Carbon (TOC) from Ruhl et al. (2010). The most common marine palynomorphs are *Micrhystridium* spp. which comprise of, on average, over 80% of the marine fraction. Both *Baltisphaeridium* spp. and *Veryhachium* spp. have low abundances and neither correlate to the ammonite zones nor the $\delta^{13}C$ values and TOC*. Leiofusa jurassica* makes up almost 40% of the marine assemblage at the base but quickly dissappears at the boundary

between the *planorbis* and *johnstoni* subzones. Dinoflagellate cysts are not common at the base of the section but become common after the *Psiloceras planorbis* and *Alsatites liasicus* ammonite zone boundary. In the *Alsatites liasicus* ammonite zone dinoflagellates show intense fluctuations on an approximately 5 meter scale between 6% and 35% relative abundance. From the boundary with the *Schlotheimia angulata* upwards dinoflagellates become a smaller, but more stable, proportion of the marine assemblage. The prasinophytes are irregularly fluctuating throughout the section and seem to correlate with lower TOC values but they do not show a significant relation with $\delta^{13}C$.

4.3 Relative Terrestrial record

Figure 9 shows the relative abundances of the terrestrial palynomorphs, again, compared to the $\delta^{13}C$ values and TOC from Ruhl et al. (2010). The most common terrestrial palynomorphs with over 80% of the terrestrial assemblage is the pollen *Classopollis*. At the base of the section, *Classopollis* is one of only three terrestrial species present. The diversity in the terrestrial fraction increases upward of the boundary between the *planorbis* and *johnstoni* subzone boundary. Sulcate pollen, *Perinopollenites* and C*erebropollenites* spp. all have low relative abundances and do not show a significant pattern. Only a small quantity of the terrestrial fraction consists of spores. The most common spore is *Kraeuselisporites* and the other spores are so uncommon that they are grouped as 'other spores'. All spores seem to show the same relative abundance pattern as *Chasmatosporites* and Bisaccate pollen, where their peak abundances have relative higher $\delta^{13}C_{org}$ values but low TOC.

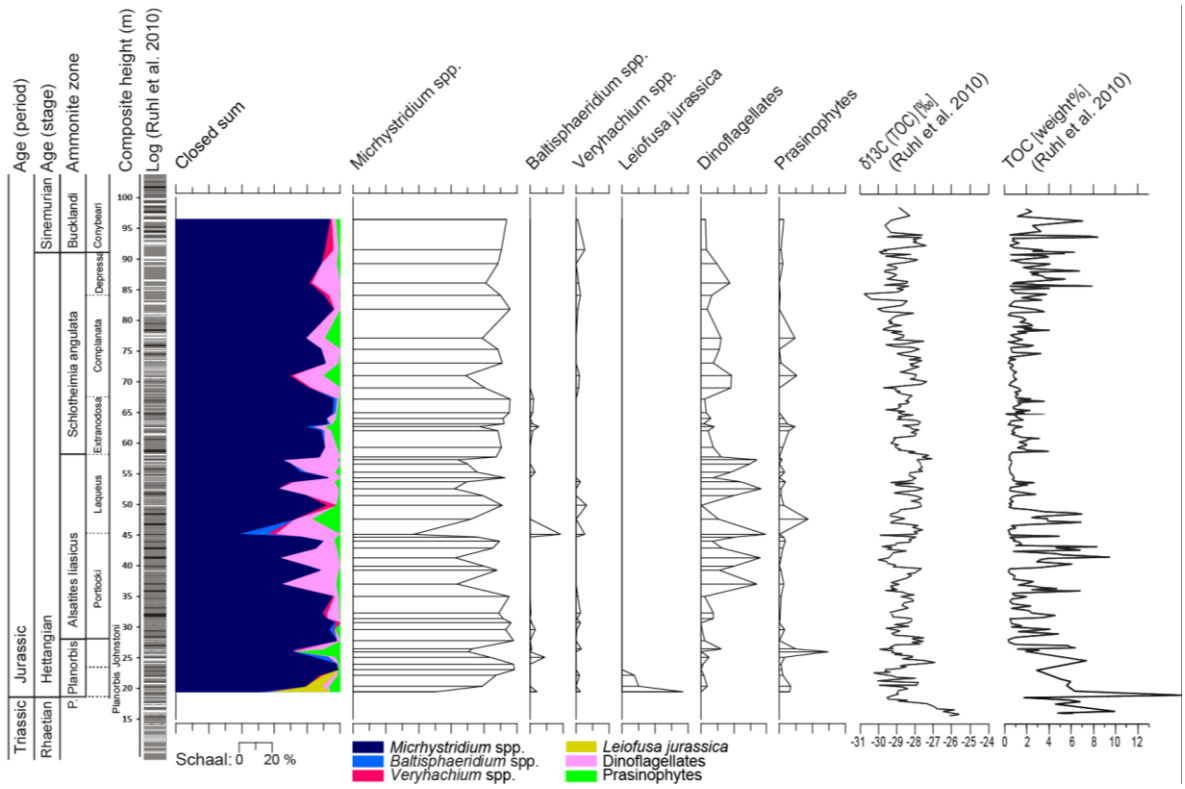

Figure 8, Relative abundance of marine species, displayed both as a closed sum plot (left) as well as separated plots (middle) together with carbon isotopes and TOC from Ruhl et al. (2010).

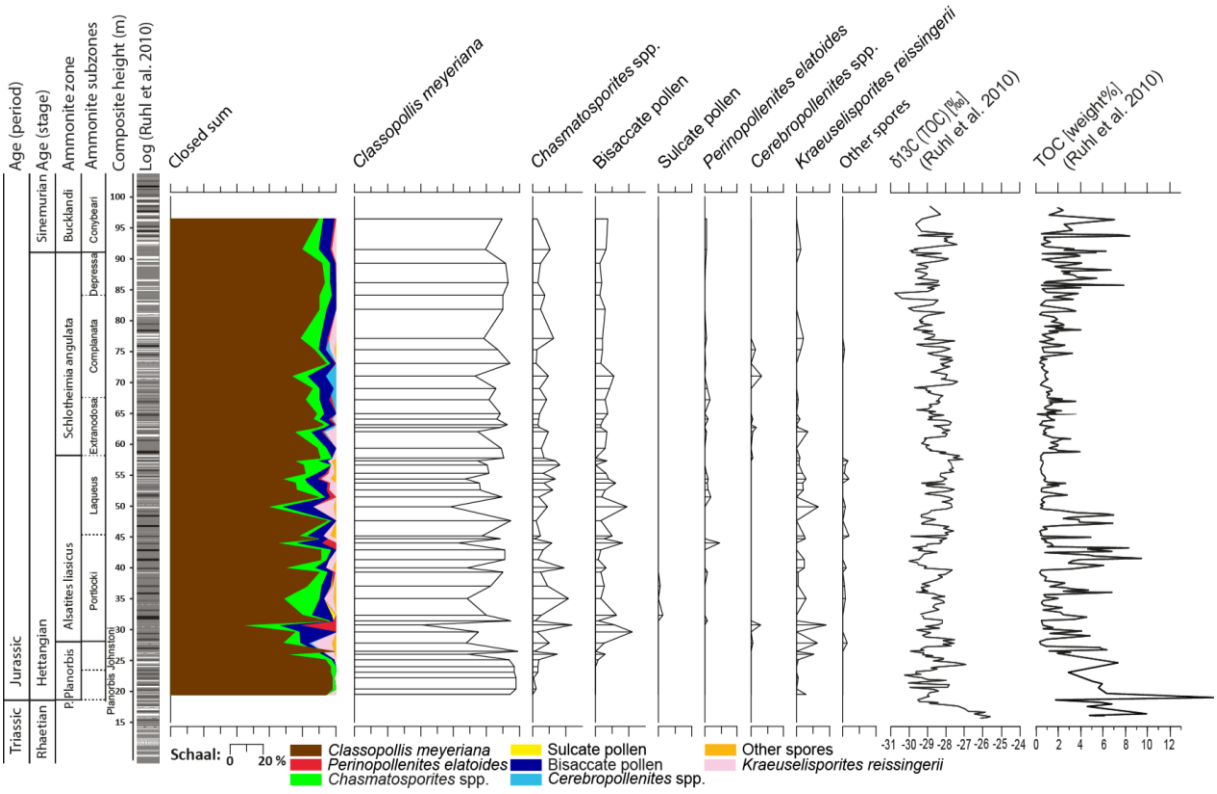

Figure 9, Relative abundance of terrestrial species, displayed both as a closed sum plot (left) as well as separated plots (middle) together with carbon isotopes and TOC from Ruhl et al. (2010).

4.4 Preservation

Figure 10 shows the marine palynomorph record and Figure 11 the terrestrial palynomorph record with absolute abundances. Lycopodium counts vary a lot and quite some slides have low lycopodium counts of under 10 lycopodium spores per approximately 300 palynomorphs. There are two samples with no lycopodium spores at all, which both are substituted by one so that absolute calculations could be made. The absolute abundances are compared with the ratio between the amount of Structureless Organic Matter (SOM) versus large amounts of pyrite. Both records show an identical pattern: when SOM is high, absolute abundances of palynomorphs are also high. When pyrite is abundant, the total amount of total palynomorhps is significantly reduced. The behaviour of the abolute abundances of palynomorphs does not seem to correlate in any way to the ammonite zones or subzones. Between 50 m and 75 m the total amount of palynomorphs is in both the marine and terrestrial record significantly reduced. High amounts of SOM do not suggest that there is no pyrite at all, every sample contains pyrite. When SOM is high the pyrite grains are tiny and with very little SOM pyrite grains can become larger and vary in size.

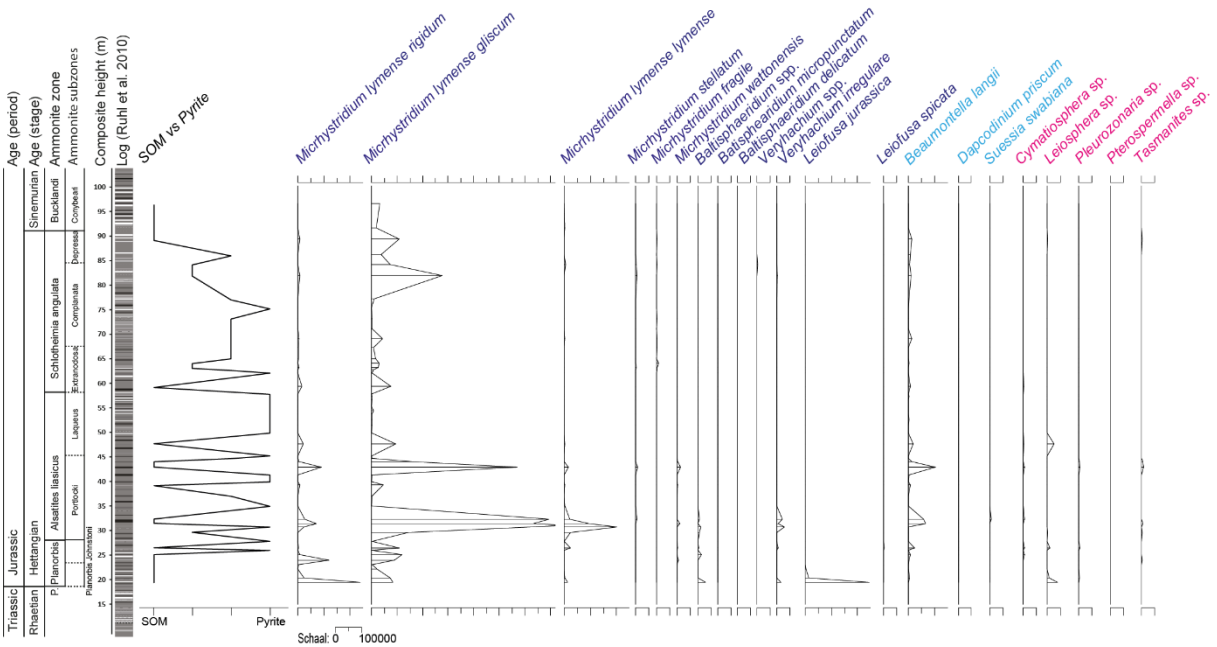

Figure 10, Absolute abundance of marine species plotted against pyrite vs SOM content. Acritarchs in dark blue, dinoflagellates in light blue and prasinophytes in pink.

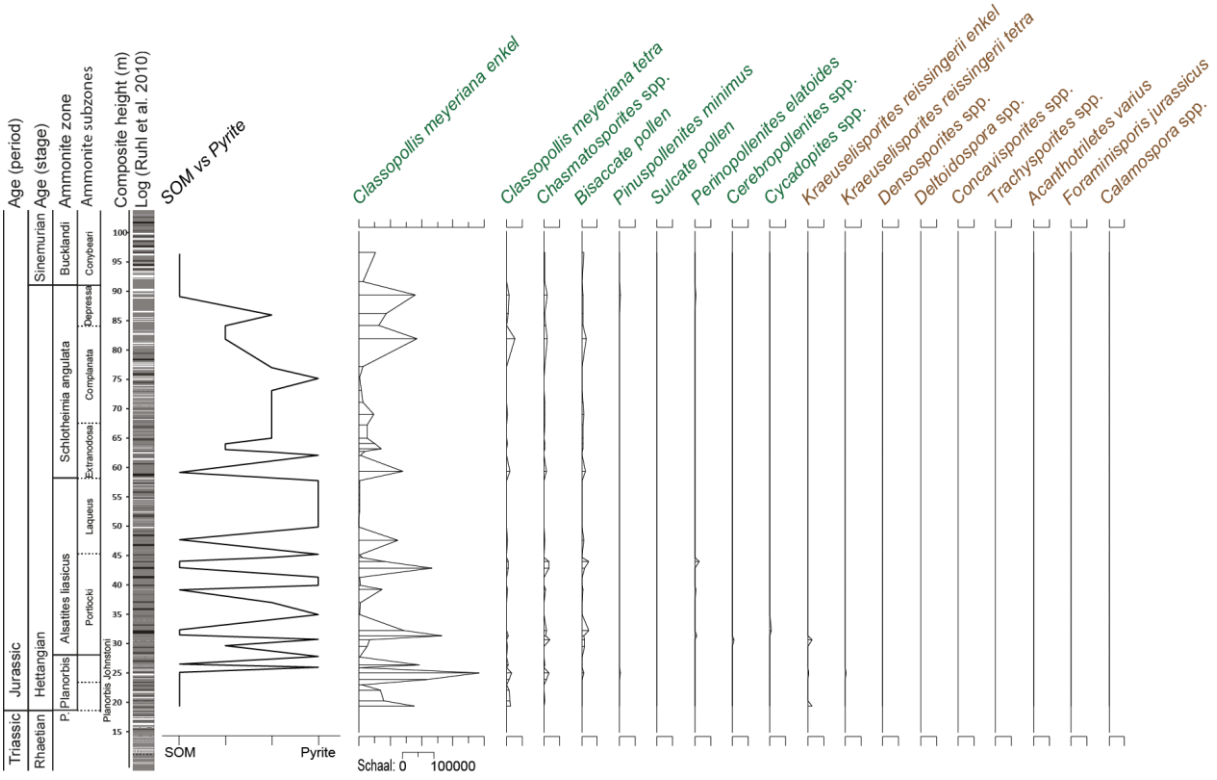

Figure 11, Absolute abundances of terrestrial species plotted against pyrite vs SOM content. Pollen in green and spores in brown.

4.5 Biodiversity

Figure 12 (top) shows three different measures for biodiversity over all palynomorphs. The evenness fluctuates between 0.45 and 0.70 indicating a rather low biodiversity. The species richness shows also fluctuations, indicating that the population is not very stable. The

Shannon-Index fluctuates around 1.5 indicating an unhealthy population. The main trend for all three methods is a slightly increasing biodiversity for the interval between 19 m and 48 m and a slightly decreasing biodiversity from 48 m up.

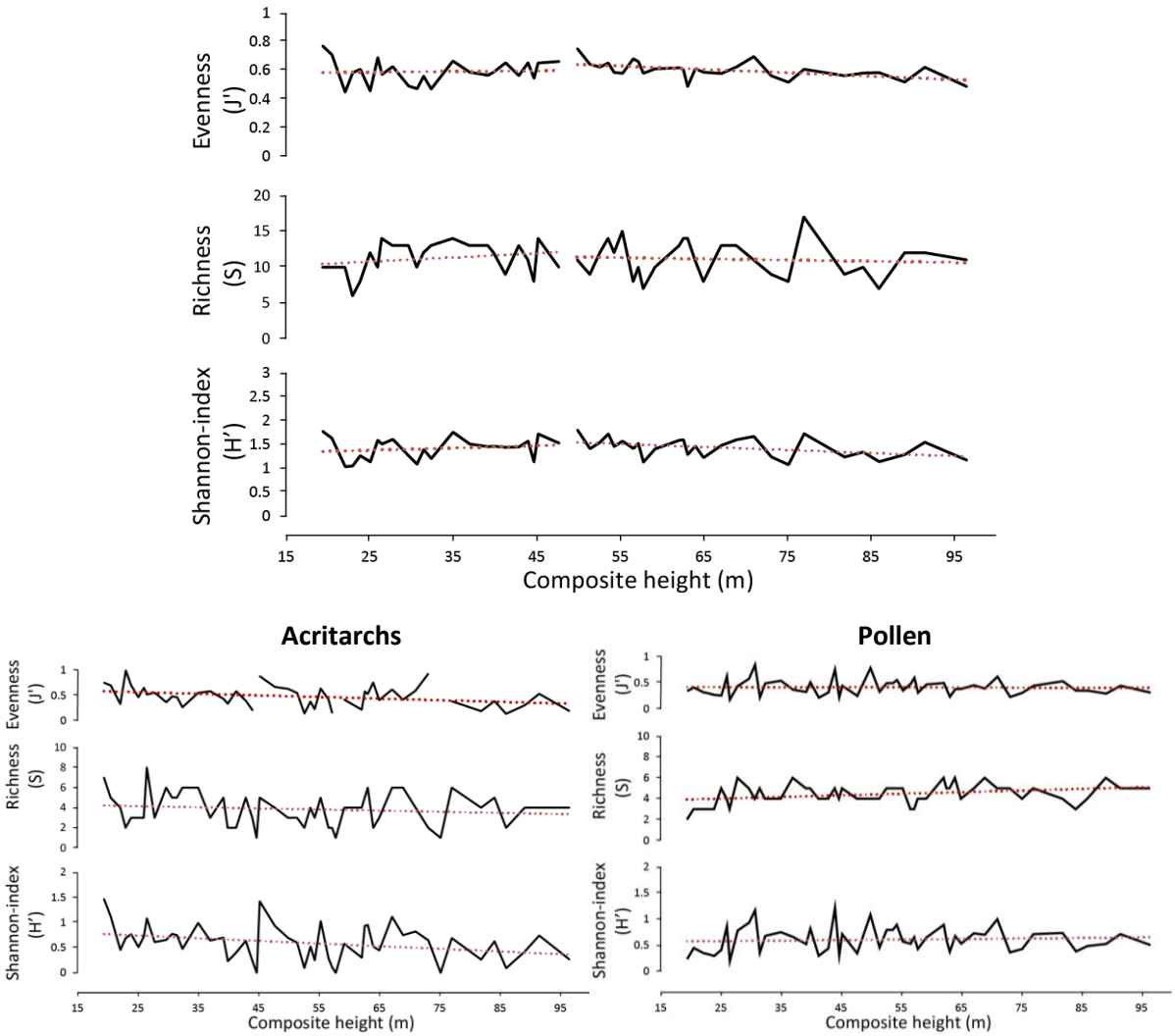

Figure 12, Top: Biodiversity indices over all palynomorphs. Bottom: Biodiversity indices of acritarchs (left) and pollen (right).

Since acritarchs and pollen were by far the largest groups of palynomorphs, they are specified in figure 12 (bottom). The acritarchs, indicative for the marine fraction, show a population which is unstable, unhealthy and low in diversity which is also declining over the entire section. In pollen, the fluctuations (especially in richness) are less extreme, indicating a more stable terrestrial environment. Although the evenness and shannon-index are relatively low they are both increasing over the entire section.

4.6 Astronomical forcing

Spectral analysis was performed on the absolute abundance of palynomorphs. Figure 13 shows two peaks in the powerspectrum with an 80% confidence interval, one peak at 5.96 meter and one peak 13.2 meter. However, instead of two cycles being present it is more likely that the longer cycle is a doubling of the shorter cycle. The spectral analysis method and

sampling resolution combined are the main reason that no cycles were found smaller than five meters.

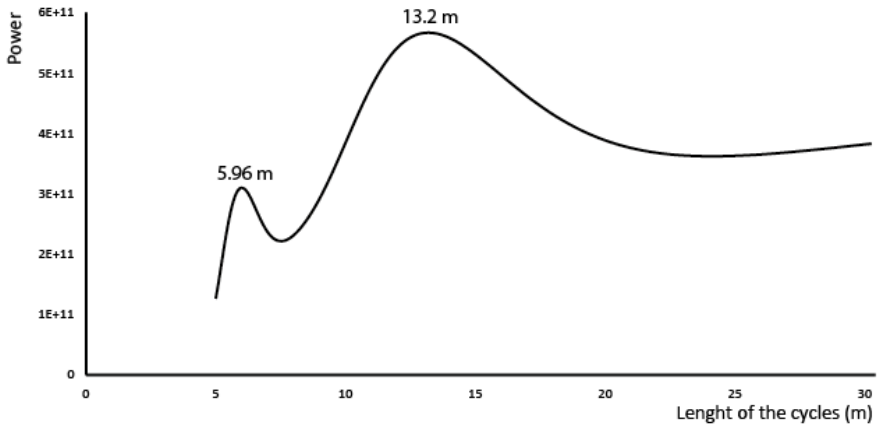

Figure 13, Powerspectrum of the absolute abundance of the total amount of palynomorphs.

The filter of the absolute abundances for both cycles can be found in Figure 14. The green graph shows the filtering of the 5.96 meter cycle and when comparing to the absolute abundances this cycle seems to correlate to every peak in the absolute abundances (purple graph). The green graph also shows a larger pattern, with higher power values in the first half, and lower values in the last part of the graph. So it seems like a larger cycle is influencing this smaller cyclicity. The blue graph shows the filtering of the 13.2 meter cycle and when comparing this filter to the absolute abundances they fit for the first two cycles, but from there it does not correlate anymore.

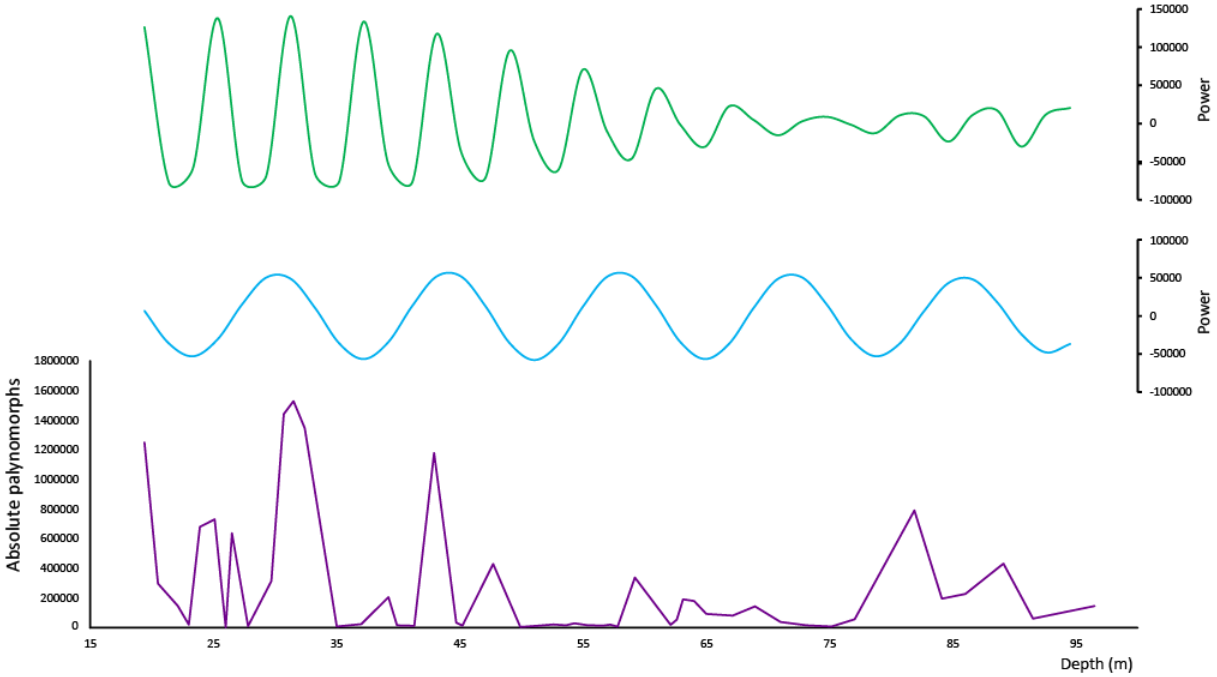

Figure 14, Below the absolute abundance of all palynomorphs (purple) with on top the 5.96 m filter in green and the 13.2 m filter in blue.

4.7 Sporomorph Ecogroups

All pollen and spores present in this section with known SEGs are described in Table 2. The most dominant sporomorph, *Classopollis*, is assigned to the Coastal SEG and is indicative for drier and warmer conditions. Other sporomorphs with a Coastal SEG are the uncommon *Densosporites* and more common *Kraeuselisporites*. *Cerebropollenites* is the only Pioneer SEG found and *Foraminisporis jurassicus* the only River SEG found. Bisaccate pollen are the only sporomorphs from the Upland SEG. All other terrestrial palynomorphs are found in the Lowland and show a both wetter/drier as well as a both warmer/cooler signal. The wetter/drier signal shows that the plains are sometimes dry and other times submerged with fresh water. The temperature and drought signals can be found in Figure 15, as well as the relative quantity of different SEGs over the entire section.

Sporomorph	**Type**	**Climate indication**	**SEG**
Cerebropollenites	Pollen		Pioneer
Classopollis	Pollen	Drier & warmer	Coastal
Chasmatosporites	Pollen	Drier & cooler	Lowland
Cycadopites	Pollen	Drier & warmer	Lowland
Bisaccate pollen	Pollen		Upland
Perinopollenites	Pollen	Wetter & cooler	Lowland
Acanthotriletes varius	Spore	Wetter	Lowland
Concavisporites	Spore	Drier & warmer	Lowland
Calamospora	Spore	Wetter & warmer	Lowland
Deltoidospora	Spore	Drier & warmer	Lowland
Densosporites	Spore		Coastal
Foraminisporis jurassicus	Spore		River
Kraeuselisporites	Spore		Coastal

Table 2, Pollen and spores with their assigned SEG (Abbink et al., 2004; Van der Weijst, 2015)

The Coastal SEG makes up the largest part of the terrestrial palynomorphs, with values of almost 100% at the base of the section. In the first ten meters the percentage drops gradually to 60%. From this point up, the amount of Coastal SEG starts to fluctuate between values of 70% and 90% of the total number of sporomorphs. From the ammonite zone boundary between *Alsatites liasicus* and *Schlotheimia angulata* up, the period of the fluctuations becomes more stretched. Both the Lowland and Upland SEG show the same pattern, starting low at the base and then slowly increasing to values around 20% in the first 10 meters. However, the Upland SEG begins only after the boundary between ammonite subzones *Planorbis* and *Johnstoni*. After the first ten meters the values of both SEGs start to fluctuate between 5% and 10-15%. From the ammonite zone boundary between *Alsatites liasicus* and *Schlotheimia angulata* up, the period of the fluctuations becomes more stretched. The River SEG and Pioneer SEG are found rarely and do not show a significant pattern. For a good

interpretation of the climate in the Early Jurassic it is best to look at the lowland SEG (Abbink et al., 2004). However, the amount of lowland species is low thus therefore the temperature signal is also plotted with over all species. The temperature plot of only the lowland species indicates a colder climate with only four peaks with warmer species. The drought plot of the lowland species indicates a dry climate with a few peaks were the climate becomes more wet. For all species, the beginning of the Jurassic has a Cool/Warm ratio of almost zero, indicating that only species with a 'warmer' climate indication are present. From 26 m up until the boundary between ammonite subzones *Portlocki* and *Laqueus* the ratio shows big fluctuations so that the amount of 'cooler' species sometimes make up over half of the total sporomorph count. After this boundary the ratio is again low and then slowly increases to a value of around 0.2. After the ammonite zone boundary between *Alsatites liasicus* and *Schlotheimia angulata* the period of the fluctuations in the ratio becomes smaller and does not get higher than 0.2.

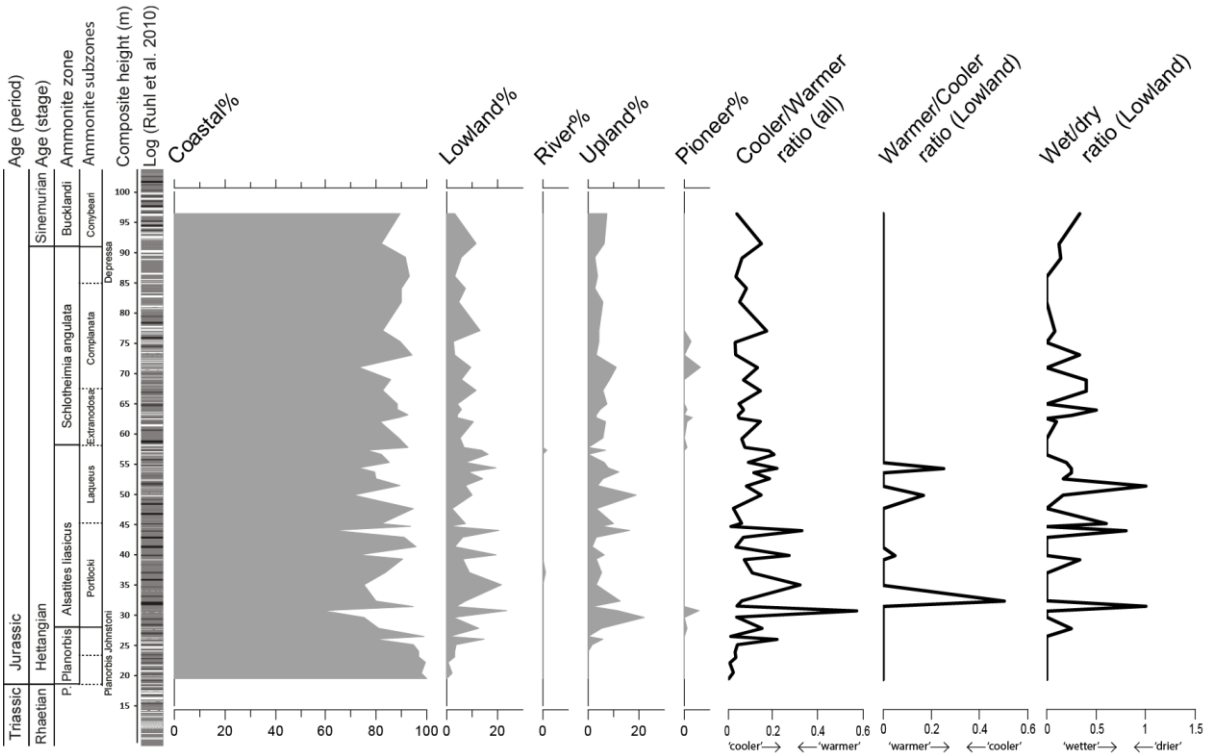

Figure 15, Stratigraphic distribution of SEGs plotted next to the cooler/warmer species ratio for all species and for only the Lowland SEG both the warmer/cooler ratio (note: this is different than for all species) and the wet/dry ratio

5. Discussion

At the end of the Triassic red algae were blooming but right after the ETE they experienced severe extinction and were replaced with green algae (van de Schootbrugge et al., 2007). Simultaneously, oceans experienced anoxic and euxinic conditions on a global scale (Damsté et al., 2001; van de Schootbrugge et al., 2007; Richoz et al., 2012; Jaraula et al., 2013; van de Schootbrugge et al., 2013; Kasprak et al., 2015). In the following section the period following the ETE event will be discussed to look for links between ocean deoxygenation and phytoplankton evolution.

5.1 Biodiversity

During the End Triassic Extinction approximately 80 % of all species went extinct (Sepkowski, 1996). To gain insights in the environmental recovery of during the Hettangian stage, multivariate statistics were used for calculations on biodiversity. Overall the biodiversity at this location is, with an average Shannon-Index of 1.5 where 3-4 is healthy, very low suggesting that the population was unhealthy. A weak population corresponds to what one expects in the aftermath of a large mass extinction. The biodiversity in the acritarchs population was already very low at the beginning of the Hettangian but halved going up in the sedimentary succession, which is suggesting that the acritarchs population becomes weaker. The diversity index of Pollen is also overall very low but show an increase in the diversity over time and therefore suggest that the population is becoming healthier but is still in a recovery phase. Overall, the biodiversity measures indicate unstable and poor conditions. The amplitude of the fluctuations is larger for acritarchs than for pollen which might indicate that the marine conditions are more dynamic than the terrestrial environment.

The use of the Shannon-Index, richness and evenness has some pitfalls when it is used as a measure for biodiversity in the past. For both the marine and terrestrial palynomorphs preservation can be an issue. The high amount of pyritization could be problematic if some species are mineralized better or faster than other species, removing them from the record and thus distorting the quantity of biodiversity. In the marine realm there was only looked at the organic palynomorphs and other micro and macro flora and fauna, hereby neglecting part of the population and thus lacking information. This is also a problem in the terrestrial realm. Furthermore, pollen and spores are not in situ at the section since they were transported by water or wind, species that are less well transported might be absent in this record and therefore disrupt the amount of biodiversity.

5.2 Organic matter preservation

Pyrite is a mineral that is commonly present in organic rich sediments and can be used for detecting oxygen poor conditions (Berner, 1984; Raiswell & Berner, 1985; Raiswell et al., 1988; Wignall & Newton, 1998). The size of pyrite framboids range with the oxygenation state of the water column. Pyrite in organic rich sedimentary depositions can be formed in two different ways (Wignall & Newton, 1998). First of all, pyrite can be formed after organic matter deposition. This needs anoxic sediments, where sulphate reducing bacteria create euxinic conditions and also oxic or dysoxic bottom water conditions (Raiswell, 1982; Fisher & Hudson, 1987; Canfield & Thamdrup, 1994). These conditions can create various sizes of pyrite framboids but also more euhedral crystals and nondescript solid matters (Wilkin et al., 1996). This pyrite formation is related to low productivity and slow burial, therefore there is more time for organic matter to be transformed after deposition and thus higher amounts of pyrite (Wignall & Newton, 1998). Second, pyrite framboids can be formed in the water column, before deposition. This need anoxic water column conditions and free hydrogen sulphide (Rickard, 1997) and happens just beneath the redox boundary. These conditions create tiny

framboids, only several microns in diameter, and do not range in size (Wilkin et al., 1996). Pyrite formation is related with a high productivity and fast burial since the organic matter and pyrite framboids are not transformed after deposition. (Wignall & Newton, 1998)

In this study, pyrite was found in all samples. There were samples with a high pyrite content which contained large pyrite pieces and framboids. Those samples had low palynomorph counts in both marine and terrestrial environment and contained little or no SOM (Figure 10 and Figure 11). This suggest that there was likely a low productivity during deposition and that pyrite was formed after deposition. However, the low absolute abundances can also be the result of the pyrite formation since a large part of palynomorphs are converted to pyrite. The other samples contained high amounts of SOM and only small pyrite framboids. Those samples had very high palynomorph counts in both the marine and terrestrial environment (Figure 10 and Figure 11). The high palynomorph counts and only small pyrite framboids suggest that there was a high productivity and rapid burial. The small framboids indicate that there were euxinic water column conditions.

At the base of the Hettangian the samples contained a lot of SOM and the palynomorph fraction consist of only green algae, suggesting ongoing anoxic or euxinic conditions. With the disappearance of *Leiofusa jurassica* on the boundary of the *Planorbis* and *Johnstoni* ammonite subzones, pyrite first appears in the samples suggesting a shift in the redox conditions, however *Beaumontella,* a dinoflagellate, remains low. From here up, the amount of pyrite and SOM in the samples starts to fluctuate, together with relative amount of acritarchs versus dinoflagellates suggesting fluctuating oxic and anoxic/euxinic conditions. From approximately 50 meters upwards more stable conditions occur, with low absolute abundances and a high pyrite content suggesting a relative stable and more oxic environment, however the relative amount of dinoflagellates still varies. The end of the Hettangian and early Sinemurian is featured with an increase in absolute abundances, less dinoflagellates and more SOM proposing a new period with high productivity and low oxygen content or possibly euxinic conditions.

5.3 Marine phytoplankton evolution

The shift from red algae towards green algae during the ETE (Falkowski et al., 2004) already indicated that red-lineaged algae flourish with a more oxic water column and that the green algae thrive under anoxic or even euxinic conditions (Van de Schootbrugge et al., 2007). During the entire Hettangian, green algae are relatively abundant suggesting that oxygen is limited and the oceans may have been poisonous. The only red algae that is still present in the Somerset samples is a dinoflagellate type *Beaumontella* spp. and this species could be indicative for more oxic conditions. For a better understanding of the recovery of the marine environment after the ETE it is useful to gain a better insight in oxygen conditions during the Hettangian in SW England. This can be done by the use of biogeochemical proxies such as isorenieratane or isorenieratane derivatives (Jaraula et al., 2013). Isorenieratane is a

biomarker produced by green sulphur bacteria which need both light and free hydrogen sulphide for growth. Therefore, isorenieratane is a proxy for euxinic conditions in the photic zone (Damsté et al., 2001). Richoz et al. (2012) looked for isorenieratane in the Hettangian in two cores in Germany and Luxemburg. Both cores contained several peaks of isorenieratane, suggesting episodic euxinia throughout the entire Hettangian stage. Jaraula et al. (2013) found a peak of isorenieratane at the base of the Hettangian in St. Audries Bay. At the *Planorbis* and *Johnstoni* ammonite subzone boundary no isorenieratane was found. This confirms the assumption that the samples containing SOM with small pyrite framboids at the base of the Hettangian were formed with euxinic conditions and the samples with a high pyrite content were formed when there was no photic zone euxinia. The results from this study therefore also indicate episodic euxinia during the Hettangian.

5.4 Terrestrial recovery

In the terrestrial realm the ETE event is characterized by a displacement of arborescent vegetation which is widely replaced by ferns and fern allies. Hereafter, the Hettangian stage is populated by Cheirolepidiaceae and Taxodiceae conifers like *Classopollis*, *Perionopollenites elatoides* and *Pinuspollenites minimus* and the recovery is accompanied by Kraeuselisporites (Van de Schootbrugge et al., 2009). The palynology at the end of the Triassic in St. Audries bay was already studied by Bonis et al. (2010; 2012) and reveals that quite some conifers, seed ferns and gymnosperms rapidly are replaced by club mosses and ferns. At the Triassic-Jurassic transition the changes in palynomorphs are already reset and the terrestrial population is dominated by over 80% of Cheirolepidiaceae. This study starts after the Triassic-Jurassic transition and therefore no fern spores were found. The entire *planorbis* ammonite subzone is characterized by mainly *Classopollis* and few *Chasmatosporites* and *Kraeuselisporites*. Similar as to the marine palynomorphs, after the *Planorbis* and *Johnstoni* ammonite subzones boundary the variety in terrestrial palynomorphs increases, which suggests that they do experience the similar environmental changes. Hereafter the terrestrial palynomorphs only fluctuate with a small percentage implying that the terrestrial realm remains relative stable during the remainder of the Hettangian.

The SEG model and the relative abundance of terrestrial palynomorphs show similar patterns (Figure 11 and Figure 15), which makes sense since only one type of Pollen is very abundant. The Coastal SEG is mainly alternating with the Lowland SEG, which, according to Abbink et al. (2004) implies fluctuations in the relative sea level. Therefore, fluctuations in the relative abundance of species can be the result of small, local, sea level variations. Abbink et al. (2004) stated that climate variations are best preserved in the Lowland SEG. This research however is low on Lowland species and therefore provides temperature results that one should not expect for the Hettangian, since the Early Jurassic is known for strong greenhouse warming and thus higher temperatures. Though, results here presented for the Lowland SEG only show a temperature ratio indicating a ‘colder’ climate, therefore it was decided to also look at the temperature variations over all species. The changes in temperature over all terrestrial

palynomorphs show a much warmer signal with a ratio fluctuating between 0 and 0.2 indicating that the 'warmer' species were dominant and thus that the Hettangian featured a warm climate. The wet/dry ratio of the Lowland SEG shows that the lowland is experiencing a relative dry climate. However, there are several 'wet' peaks which are thought to represent fresh water flooding of the Lowland.

5.5 Astronomical forcing

Since both Ruhl et al. (2010) and Hüsing et al. (2014) found evidence for astronomical forcing during the Hettangian in SW England, it is plausible that there could be cyclicity in the presence of marine and terrestrial palynomorphs. Ruhl et al. (2010) and Hüsing et al. (2014) both found short cycles between 3.8 and 5.8 meters that are probably the 100 kyr eccentricity cycle. This study only found a peak approximately every 5.9 meters which could be (due to a low resolution) the upper limit of this 100 kyr eccentricity cycle. Unfortunately, the sampling resolution for this study was too low to find any cyclicity under 5 meters. Therefore, for a more reliable result a higher resolution palynology study is advised. However, when we assume that the 5.9-meter cycle is indeed the 100 kyr eccentricity cycle, then the amount of SOM and pyrite in the samples is astronomically forced and thus anoxic/euxinic water column conditions are eccentricity forced. Schmincke (2004) suggests that volcanic forcing usually overprints astronomical climate forcing effects, but that it is possible for astronomical climate forcing to exceed the volcanic forcing. For the Hettangian it is convincingly that volcanic activity was a large contributor to anoxic/euxinic conditions. However, the cyclicity found by Ruhl et al. (2010) and Hüsing et al. (2014) suggests that there also is an astronomical effect. The astronomical forcing likely exerts an additional influence on the water column conditions and therefore it could be the main cause for changes of the redox state of the oceans.

5.6 Broad perspective and implications

Estimates on the duration of the CAMP volcanism are limited to approximately 600 kyr and only four eruptive events from North America and Morocco have been dated so far. (Blackburn et al., 2013) This study, however, show that the marine environment was still disrupted at the end of the Hettangian so perhaps the volcanic activity continued for a longer period. The CAMP extended from South America to North America, West Africa and Iberia, and large parts are still unexplored. An investigation on the lava's in South America and Iberia might reveal ongoing volcanic activity with corresponding pulses of CO_2 and H_2S in the late Hettangian and early Sinemurian.

Large climate change events in the past are probably the best proxy to predict the effect of the present-day human-induced climate change. McElwain et al. (1999) stated that during the ETE the CO_2 concentrations of the atmosphere started of around 600ppm and quadrupled to approximately 2400ppm, which caused a global temperature rise of 4°C and salinity decreased with 3 PSU (van de Schootbrugge et al., 2007). Today, CO_2 concentrations have already rose from 280ppm (preindustrial value) to over 400ppm. This increase has already lead to an

increase in acidification of the Earth's oceans. The latest IPCC report predicts, in a worst case scenario, that around the year 2100 the pre-industrial CO_2 concentrations in the atmosphere have also quadrupled to over 1000ppm and that this coincides with a global temperature rise of also 4°C. When this same rise in temperature really happens, it possibly also enhances the hydrological cycle, causing stratification of the water column and therefore anoxic conditions similar to the ETE event. This creates the possibility of a human-induced mass extinction event. However, there are also numerous differences between the situation at the end of the Triassic and present-day. For example, nowadays the land masses covering the Earth are distributed differently, therefore the present-day hydrological cycle is different and should have a dissimilar effect. Also, both the CO_2 concentration and global temperature were much higher in the past, making it likely that the outcome will be different.

6. Conclusions

The end Triassic extinction event was most likely a combination of circumstances caused by extensive CAMP volcanism. Especially ocean acidification, an increase in global temperature, inducing an enhanced hydrological cycle and therefore stratification, anoxic oceans and H_2S poisoning on both land and in the ocean were major consequences of this large igneous province. In this study, the high abundances of green algae through the entire succession implicate that the ocean conditions remained dysoxic during the Hettangian. Furthermore, fluctuations in the amount of pyrite and SOM suggested that there also were episodes with ongoing euxinic water column conditions during the first stage of the Jurassic. The shifting redox conditions were most likely a result of ongoing volcanism, much longer than previously thought. There is also evidence that these shifting redox conditions can be linked to astronomical forcing, were eccentricity is affecting oxygen conditions of the water column. During the Hettangian, the terrestrial realm seems to be scarcely influenced with a relative stable palynomorph composition which confirms the idea that the terrestrial environment recovers faster than the marine environment. For future investigations on the climate recovery during the Hettangian quite some improvements are suggested. A higher resolution study is needed for a better understanding the role of astronomical forcing on the water column conditions. To discover whether the Hettangian really did experience euxinic episodes a biogeochemical study is suggested to measure the proxy for euxinia: isorenieratane. And last, to gain more insight in the duration and magnitude of the CAMP volcanism more lavas and magmas should be investigated. The current rise in the global CO_2 concentrations for the next hundred years predicts a similar temperature rise as the Hettangian stage. Therefore, the early Jurassic might be a good analogue for the future of our planet.

Acknowledgements

Most important, I want to express my appreciation to both Bas van de Schootbrugge and Sander Houben for giving me the opportunity to work on this project. I want to thank them for introducing me to the Early Jurassic, taking me on their fieldtrip to the wonderful Jurassic Coast in SW England and helping me out with the endless amount of my questions. Further, I would like to thank Natasja Welters for teaching me to find my way around the laboratory and Nico Janssen for helping me process all the samples. I want to thank Peter Bijl for giving me a short introduction on how to process palynologic data and Sabine Gollner for helping me out with calculations on the biodiversity. Furthermore, Frits Hilgen was a great help for brushing up on my knowledge on astronomical climate forcing. And last, but definitely not least, I would like to thank all students, and new friends, from the student room, for endless discussions, laughter and coffee breaks which kept me going during this project.

References

Abbink, O. A. (1998). Palynological investigations in the Jurassic of the North Sea region. Laboratory of Palaeobotany and Palynology Contribution Series Nr. 8. LPP Foundation, Utrecht, 1–191 p.

Abbink, O. A., Van Konijnenburg-Van Cittert, J. H. A., & Visscher, H. (2004). A sporomorph ecogroup model for the Northwest European Jurassic–Lower Cretaceousi: concepts and framework. Netherlands Journal of Geosciences/Geologie en Mijnbouw, 83(1).

Beerling, D. J., & Berner, R. A. (2002). Biogeochemical constraints on the Triassic-Jurassic boundary carbon cycle event. Global Biogeochemical Cycles, 16(3).

Berner, R. A. (1984). Sedimentary pyrite formation: an update. Geochimica et cosmochimica Acta, 48(4), 605-615.

Blackburn, T. J., Olsen, P. E., Bowring, S. A., McLean, N. M., Kent, D. V., Puffer, J., ... & Et-Touhami, M. (2013). Zircon U-Pb geochronology links the End-Triassic extinction with the Central Atlantic Magmatic Province. Science, 340(6135), 941-945.

Blakey, R., Colorado Plateau Geosystems, Arizona USA, Paleogeographic map downloaded from: http://cpgeosystems.com/paleomaps.html

Bonis, N. R., Kürschner, W. M., & Krystyn, L. (2009). A detailed palynological study of the Triassic–Jurassic transition in key sections of the Eiberg Basin (Northern Calcareous Alps, Austria). Review of Palaeobotany and Palynology, 156(3), 376-400.

Bonis, N. R., Ruhl, M., & Kürschner, W. M. (2010). Milankovitch-scale palynological turnover across the Triassic–Jurassic transition at St. Audrie's Bay, SW UK. Journal of the Geological Society, 167(5), 877-888.

Bonis, N. R., & Kürschner, W. M. (2012). Vegetation history, diversity patterns, and climate change across the Triassic/Jurassic boundary. Paleobiology, 38(2), 240-264.

Canfield, D. E., & Thamdrup, B. (1994). The production of (34) S-depleted sulfide during bacterial disproportionation of elemental sulfur. Science, 266(5193), 1973.

Colwell, R. K. (2009). "Biodiversity: Concepts, Patterns and Measurement". In Simon A. Levin. The Princeton Guide to Ecology. Princeton: Princeton University Press. pp. 257–263

Damsté, J. S. S., Schouten, S., & van Duin, A. C. (2001). Isorenieratene derivatives in sediments: possible controls on their distribution. Geochimica et Cosmochimica Acta, 65(10), 1557-1571.

Falkowski, P. G., Katz, M. E., Knoll, A. H., Quigg, A., Raven, J. A., Schofield, O., & Taylor, F. J. R. (2004). The evolution of modern eukaryotic phytoplankton. science, 305(5682), 354-360.

Fisher, I. S. J., & Hudson, J. D. (1987). Pyrite formation in Jurassic shales of contrasting biofacies. Geological Society, London, Special Publications, 26(1), 69-78.

Hallam, A. (1990). The end-Triassic mass extinction event. Geological Society of America Special Papers, 247, 577-584.

Hallam, A. (1997). Estimates of the amount and rate of sea-level change across the Rhaetian—Hettangian and Pliensbachian—Toarcian boundaries (latest Triassic to early Jurassic). Journal of the Geological Society, 154(5), 773-779.

Hallam, A. (1998). Mass extinctions in Phanerozoic time. Geological Society, London, Special Publications, 140(1), 259-274.

Hallam, A., & Wignall, P. B. (1997). Mass extinctions and their aftermath. Oxford University Press, UK.

Hallam, A., & Wignall, P. B. (1999). Mass extinctions and sea-level changes. Earth-Science Reviews, 48(4), 217-250.

Hallam, A., Wignall, P. B., Yin, J., & Riding, J. B. (2000). An investigation into possible facies changes across the Triassic–Jurassic boundary in southern Tibet. Sedimentary Geology, 137(3), 101-106.

Hautmann, M., Benton, M. J., & Tomašových, A. (2008). Catastrophic ocean acidification at the Triassic-Jurassic boundary. Neues Jahrbuch für Geologie und Paläontologie-Abhandlungen, 249(1), 119-127.

Hesselbo, S. P., Robinson, S. A., Surlyk, F., & Piasecki, S. (2002). Terrestrial and marine extinction at the Triassic-Jurassic boundary synchronized with major carbon-cycle perturbation: A link to initiation of massive volcanism?. Geology, 30(3), 251-254.

Hesselbo, S. P., Robinson, S. A., & Surlyk, F. (2004). Sea-level change and facies development across potential Triassic–Jurassic boundary horizons, SW Britain. Journal of the Geological Society, 161(3), 365-379.

Heunisch, C., Luppold, F.W., Reinhardt, L. & Röhling, H.-G. (2010): Palynofazies, Bio- und Lithostratigrafi e im Grenzbereich Trias/Jura in der Bohrung Mariental 1 (Lappwaldmulde, Ostniedersachsen). Z. dt. Ges. Geowiss., 161: 51–98

Hüsing, S. K., Beniest, A., van der Boon, A., Abels, H. A., Deenen, M. H. L., Ruhl, M., & Krijgsman, W. (2014). Astronomically-calibrated magnetostratigraphy of the Lower Jurassic marine successions at St. Audrie's Bay and East Quantoxhead (Hettangian–Sinemurian; Somerset, UK). Palaeogeography, Palaeoclimatology, Palaeoecology, 403, 43-56.

Jaraula, C. M., Grice, K., Twitchett, R. J., Böttcher, M. E., LeMetayer, P., Dastidar, A. G., & Opazo, L. F. (2013). Elevated pCO2 leading to Late Triassic extinction, persistent photic zone euxinia, and rising sea levels. Geology, 41(9), 955-958.

Kasprak, A. H., Sepúlveda, J., Price-Waldman, R., Williford, K. H., Schoepfer, S. D., Haggart, J. W., ... & Whiteside, J. H. (2015). Episodic photic zone euxinia in the northeastern Panthalassic Ocean during the End-Triassic extinction. Geology, 43(4), 307-310.

Laskar, J., Fienga, A., Gastineau, M., & Manche, H. (2011a). La2010: a new orbital solution for the long-term motion of the Earth. Astronomy & Astrophysics, 532, A89.

Laskar, J., Gastineau, M., Delisle, J. B., Farrés, A., & Fienga, A. (2011b). Strong chaos induced by close encounters with Ceres and Vesta. Astronomy & Astrophysics, 532, L4.

Litchman, E., Klausmeier, C. A., Miller, J. R., Schofield, O. M., & Falkowski, P. G. (2006). Multi-nutrient, multi-group model of present and future oceanic phytoplankton communities. Biogeosciences Discussions, 3(3), 607-663.

Marzoli, A., Renne, P. R., Piccirillo, E. M., Ernesto, M., Bellieni, G., & De Min, A. (1999). Extensive 200-million-year-old continental flood basalts of the Central Atlantic Magmatic Province. Science, 284(5414), 616-618.

McElwain, J. C., Beerling, D. J., & Woodward, F. I. (1999). Fossil plants and global warming at the Triassic-Jurassic boundary. Science, 285(5432), 1386-1390.

McHone, J. G. (1996). Broad-terrane Jurassic flood basalts across northeastern North America. Geology, 24(4), 319-322.

Mulder, C. P. H., Bazeley-White, E., Dimitrakopoulos, P. G., Hector, A., Scherer-Lorenzen, M., & Schmid, B. (2004). Species evenness and productivity in experimental plant communities. Oikos, 107(1), 50-63.

Newell, N. D. (1963). Crises in the history of life. Scientific American, 208, 76-93.

Olsen, P. E., Kent, D. V., Sues, H. D., Koeberl, C., Huber, H., Montanari, A., ... & Hartline, B. W. (2002). Ascent of dinosaurs linked to an iridium anomaly at the Triassic-Jurassic boundary. Science, 296(5571), 1305-1307.

Paillard, D., Labeyrie, L., & Yiou, P. (1996). Macintosh program performs time-series analysis. Eos, Transactions American Geophysical Union, 77(39), 379-379.

Pálfy, J., Demény, A., Haas, J., Hetényi, M., Orchard, M. J., & Veto, I. (2001). Carbon isotope anomaly and other geochemical changes at the Triassic-Jurassic boundary from a marine section in Hungary. Geology, 29(11), 1047-1050.

Paul, C. R. C., Allison, P. A., & Brett, C. E. (2008). The occurrence and preservation of ammonites in the Blue Lias Formation (lower Jurassic) of Devon and Dorset, England and their palaeoecological, sedimentological and diagenetic significance. Palaeogeography, Palaeoclimatology, Palaeoecology, 270(3), 258-272.

Raiswell, R. (1982). Pyrite texture, isotopic composition and the availability of iron. American Journal of Science, 282(8), 1244-1263.

Raiswell, R., & Berner, R. A. (1985). Pyrite formation in euxinic and semi-euxinic sediments. American Journal of Science, 285(8), 710-724.

Raiswell, R., Buckley, F., Berner, R. A., & Anderson, T. F. (1988). Degree of pyritization of iron as a paleoenvironmental indicator of bottom-water oxygenation. Journal of Sedimentary Research, 58(5), 812-819.

Raup, D. M., & Sepkoski Jr, J. J. (1982). Mass extinctions in the marine fossil record. Science, 215(4539), 1501-1503.

Richoz, S., van de Schootbrugge, B., Pross, J., Püttmann, W., Quan, T. M., Lindström, S., ... & Hauzenberger, C. A. (2012). Hydrogen sulphide poisoning of shallow seas following the End-Triassic extinction. Nature Geoscience, 5(9), 662-667.

Rickard, D., & Luther, G. W. (1997). Kinetics of pyrite formation by the H 2 S oxidation of iron (II) monosulfide in aqueous solutions between 25 and 125 C: The mechanism. Geochimica et Cosmochimica Acta, 61(1), 135-147.

Ruhl, M., Deenen, M. H. L., Abels, H. A., Bonis, N. R., Krijgsman, W., & Kürschner, W. M. (2010). Astronomical constraints on the duration of the early Jurassic Hettangian stage and recovery rates following the end-Triassic mass extinction (St Audrie's Bay/East Quantoxhead, UK). Earth and Planetary Science Letters, 295(1), 262-276.

Ruhl, M., Bonis, N. R., Reichart, G. J., Damsté, J. S. S., & Kürschner, W. M. (2011). Atmospheric carbon injection linked to End-Triassic mass extinction. Science, 333(6041), 430-434.

Schminke, H.U. (2004). Volcanism. Berlin Heidelberg, Germany: Springer-Verlag

Seinfeld, J.H. & Pandis, S.N.. (2016) Atmospheric chemistry and physics. Hoboken, New Jersey: John Wiley & Sons

Sepkoski Jr, J. J. (1996). Patterns of Phanerozoic extinction: a perspective from global data bases. In Global events and event stratigraphy in the Phanerozoic (pp. 35-51). Springer Berlin Heidelberg.

Shannon, C.E. & Weaver, W. (1949) The mathematical theory of communication. The University of Illinois Press, Urbana, 117pp

Shannon, C.E. (1948) A mathematical theory of communication. Bell System Technical Journal, 27, 379–423

Spellerberg, I. F., & Fedor, P. J. (2003). A tribute to Claude Shannon (1916–2001) and a plea for more rigorous use of species richness, species diversity and the 'Shannon–Wiener'Index. Global ecology and biogeography, 12(3), 177-179.

Stanley, S.M.. (2009) Earth System History. New York, NY: W. H. Freeman and Company.

Tanner, L. H., Lucas, S. G., & Chapman, M. G. (2004). Assessing the record and causes of Late Triassic extinctions. Earth-Science Reviews, 65(1), 103-139.

Van de Schootbrugge, B., Tremolada, F., Rosenthal, Y., Bailey, T. R., Feist-Burkhardt, S., Brinkhuis, H., ... & Falkowski, P. G. (2007). End-Triassic calcification crisis and blooms of organic-walled 'disaster species'. Palaeogeography, Palaeoclimatology, Palaeoecology, 244(1), 126-141.

Van de Schootbrugge, B., Bachan, A., Suan, G., Richoz, S., & Payne, J. L. (2013). Microbes, mud and methane: cause and consequence of recurrent Early Jurassic anoxia following the end-Triassic mass extinction. Palaeontology, 56(4), 685-709.

van der Weijst, C. (2015). Controls on vegetation dynamics in the wake of the end-Triassic mass extinction event. Msc Thesis, unpublished.

Wall, D. (1965). Microplankton, pollen, and spores from the Lower Jurassic in Britain. Micropaleontology, 151-190.

Ward, P. D., Haggart, J. W., Carter, E. S., Wilbur, D., Tipper, H. W., & Evans, T. (2001). Sudden productivity collapse associated with the Triassic-Jurassic boundary mass extinction. Science, 292(5519), 1148-1151.

Warrington, G., Cope, J. C. W., & Ivimey-Cook, H. C. (2008). The St Audrie's Bay–Doniford Bay section, Somerset, England: updated proposal for a candidate Global Stratotype Section and Point for the base of the Hettangian Stage, and of the Jurassic System. International Subcommission on Jurassic Stratigraphy Newsletter, 35(1), 2-66.

Weedon, G. P., Jenkyns, H. C., Coe, A. L., & Hesselbo, S. P. (1999). Astronomical calibration of the Jurassic time-scale from cyclostratigraphy in British mudrock formations. Philosophical Transactions of the Royal Society of London A: Mathematical, Physical and Engineering Sciences, 357(1757), 1787-1813.

Wignall, P. B., & Newton, R. (1998). Pyrite framboid diameter as a measure of oxygen deficiency in ancient mudrocks. American Journal of Science, 298(7), 537-552.

Wignall, Paul B., and David PG Bond. "The end-Triassic and Early Jurassic mass extinction records in the British Isles." Proceedings of the Geologists' Association 119.1 (2008): 73-84.

Wilkin, R. T., Barnes, H. L., & Brantley, S. L. (1996). The size distribution of framboidal pyrite in modern sediments: an indicator of redox conditions. Geochimica et Cosmochimica Acta, 60(20), 3897-3912,

Appendix

1. Acritarchs

1. *Leiofusa jurassica*, 2. *Micrhystridium lymense rigidum*, 3. *Micrhystridium lymense gliscum*, 4. *Micrhystridium lymense lymense*, 5. *Micrhystridium fragile*, 6. *Micrhystridium stellatum* 7. *Micrhystridium wattonensis*, 8. *Veryhachium* spp.

1

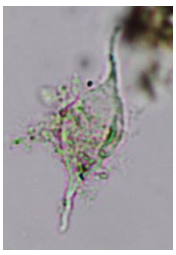

1: 50 µm

2

3

2-8: 50 µm

4

5

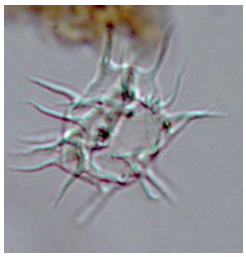

6

7

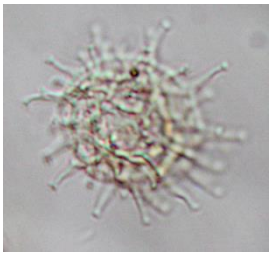

8

2. Dinoflagellates

1. *Beaumontella langii*, 2. *Dapcodinium priscum*, 3. *Suessia swabiana*

1

2

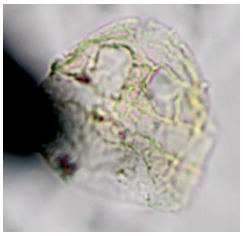

3

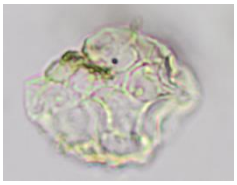

50 µm

3. Prasinophytes

1. *Cymatiosphera* sp., 2. *Pleurozonaria* sp., 3. *Pterospermella* sp., 4. *Tasmanites* sp.

1

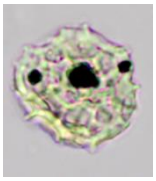

50 µm

2

3

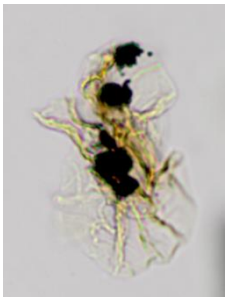

4

4. Pollen

1. Ce*rebropollenites* spp., 2. *Chasmatosporites* spp., 3. *Classopollis meyeriana* (single), 4. *Classopollis meyeriana* (tetraeder), 5. *Cycadopites* spp., 6. Sulcate pollen

1.

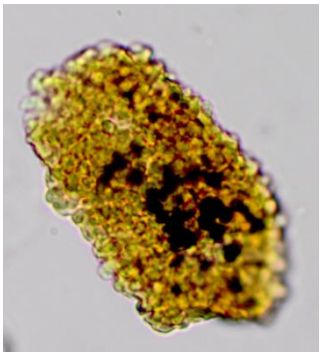

2.

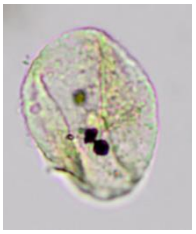

3.

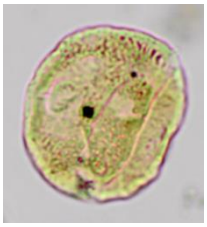

4.

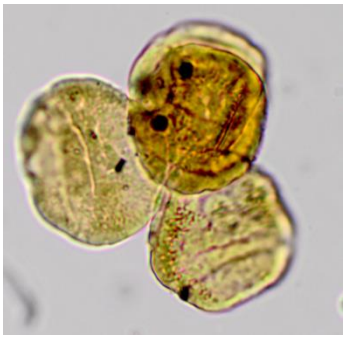

5.

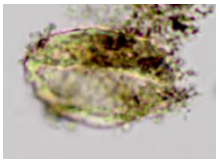

6.

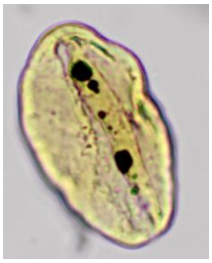

50 µm

5. Spores

1. *Acanthotriletes varius*, 2. *Calamospora* spp., 3. *Concavisporites* spp., 4. *Deltoidospora* spp., *5. Densosporites* spp., 6. *Foraminisporis jurassicus*, 7. *Kraeuselisporites reissingerii* (tetraeder), 8. *Trachysporites* spp.

1

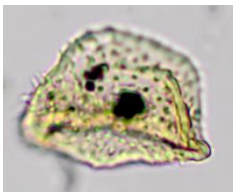

2

3

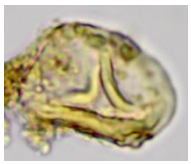

4

5

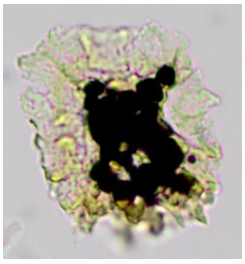

50 µm

6

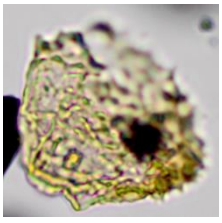

7

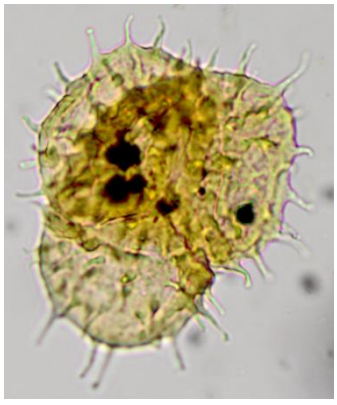

8